

The Salinity Effect in a Mixed Layer Ocean Model

JAMES R. MILLER¹

Goddard Institute For Space Studies, NASA, New York, N. Y. 10025

(Manuscript received 7 October 1974, in revised form 8 July 1975)

ABSTRACT

A model of the thermally mixed layer in the upper ocean as developed by Kraus and Turner and extended by Denman is further extended to investigate the effects of salinity. In the tropical and subtropical Atlantic Ocean rapid increases in salinity occur at the bottom of a uniformly mixed surface layer. The most significant effects produced by the inclusion of salinity are the reduction of the deepening rate and the corresponding change in the heating characteristics of the mixed layer. If the net surface heating is positive, but small, salinity effects must be included to determine whether the mixed layer temperature will increase or decrease. Precipitation over tropical oceans leads to the development of a shallow stable layer accompanied by a decrease in the temperature and salinity at the sea surface.

1. Introduction

The upper layer of the ocean responds to changes in atmospheric parameters on a time scale of several days or less. Recent works concerned with these responses have assumed the existence of a thermally homogeneous mixed layer at the ocean surface. Kraus and Turner (1967) modeled the development of such a layer by assuming that the heat inputs at the air-sea interface and the mass entrainment at the bottom of the layer are mixed uniformly throughout the layer in a time scale short relative to the time scales of interest. The wind stress at the ocean surface generates turbulent kinetic energy which does work against the buoyancy forces, thus increasing the potential energy in the mixed layer. A model-generated discontinuity in temperature and density occurs at the bottom of the mixed layer, and the deepening rate of the mixed layer is inversely proportional to the magnitude of the density jump. The work of Kraus and Turner was extended by Denman (1973) to investigate the time-dependent behavior of the upper mixed layer of the ocean in response to varying meteorological inputs.

The theoretical model of Denman was used by Denman and Miyake (1973) to predict sea surface temperature for a 12-day period in the Pacific Ocean (145°W, 50°N). The agreement with the observed sea surface temperatures was heartening. The effect of salinity in this case was insignificant because the salinity was constant to a depth of 60 m, and the thermal mixed layer was always less than 60 m deep. In the subtropical and tropical Atlantic Ocean (25°S to

30°N), a homogeneous layer of constant salinity occurs at the surface; according to Defant (1961) the thickness of this layer is usually somewhat less than the depth of the thermal layer. At the bottom of this layer the salinity increases rapidly to a maximum, and then decreases again with depth. Profiles exhibiting this behavior will be presented. They have been obtained from the U. S. Dept. of Commerce *BOMEX Period III Upper Ocean Soundings* (hereafter referred to as BOMEX).

The purpose of this paper is to study numerically several specific cases in which the salinity distribution must be considered if the thermal characteristics of the mixed layer are to be understood. The model to be used is developed by adding an equation for the conservation of salt to Denman's model. Some observational data which include salinity jumps at the bottom of the mixed layer will be used to specify initial conditions for the model. The effect of salinity on mixed layer temperatures and depths as well as the effect of precipitation on salinity and temperature in tropical oceans will be discussed.

2. Governing equations

A one-dimensional, time-dependent model of the upper ocean developed by Kraus and Turner has been extended by Denman to include physically realistic time-dependent boundary conditions. Equations for the conservation of heat and mechanical energy are the physical basis for the model. The effect of salinity can be investigated by extending Denman's model to include an equation for the conservation of salt content. A mixed layer of depth h is assumed to be completely homogeneous with respect to temperature and salinity;

¹ Present affiliation: Department of Meteorology and Physical Oceanography, Cook College, Rutgers University, New Brunswick, N.J. 08903.

it is bounded below by fixed temperature and salinity gradients. A system of ordinary differential equations is derived which specifies the time derivatives of h , T , T_h , S and S_h as functions of the time-dependent boundary inputs. The temperature and salinity of the mixed layer are denoted by T and S , respectively; T_h and S_h denote the temperature and salinity immediately below the mixed layer. The boundary inputs include wind stress, solar and back radiation, latent and sensible heat fluxes, and the temperature and salinity gradients below the layer.

The time-averaged turbulent form of the equation for conservation of salt in the mixed layer is

$$\frac{\partial S}{\partial t} + w \frac{\partial S}{\partial z} + \frac{\partial}{\partial z} (\overline{w'S'}) = 0, \quad (1)$$

where w' and S' are fluctuating components of the vertical velocity and salinity, respectively. At the air-sea interface ($z=0$), changes in salinity occur as a result of precipitation and evaporation. At the bottom of the mixed layer, salinity changes are due to entrainment of water having a different salinity. The equations for salt fluxes at the upper and lower boundaries with $w=0$ are

$$\overline{w'S'}|_0 = S(P-E), \quad (2)$$

$$\frac{dh}{dt} = \frac{2[G-D+R\gamma^{-1}(1-e^{-\gamma h})] - h \left[B+H_e+H_s+R(1+e^{-\gamma h}) - \frac{\lambda}{\alpha} S(P-E) \right]}{h \left[(T-T_h) + \frac{\lambda}{\alpha} (S-S_h) \right]} \quad (6)$$

$$\frac{dT}{dt} = \frac{1}{h} \left[\frac{dh}{dt} (T-T_h) + B+H_e+H_s+R(1+e^{-\gamma h}) \right] \quad (7)$$

$$\frac{dT_h}{dt} = \gamma R e^{-\gamma h} - \frac{dh}{dt} L_T \quad (8)$$

$$\frac{dS}{dt} = \frac{1}{h} \left[\frac{dh}{dt} (S-S_h) - S(P-E) \right] \quad (9)$$

$$\frac{dS_h}{dt} = -\frac{dh}{dt} L_s \quad (10)$$

In the above equations ($G-D$) is the turbulent energy derived from the wind stress, R the incident solar radiation, $-B$ the net longwave back radiation from the sea surface, and H_s and H_e are the sensible and latent heat fluxes, respectively. The evaporation E is proportional to the latent heat flux. At the bottom of the mixed layer, the temperature and salinity gradients are denoted by L_T and L_s , respectively. When $\lambda=0$, the equations for h , T and T_h are equivalent to

$$\overline{w'S'}|_h = -\frac{dh}{dt} (S-S_h). \quad (3)$$

Precipitation and evaporation rates (mm h^{-1}) are denoted by P and E , respectively, and dh/dt is the rate at which the mixed layer deepens. Eq. (1) is integrated over the depth of the mixed layer to obtain

$$h \frac{dS}{dt} + \frac{dh}{dt} (S-S_h) + S(P-E) = 0. \quad (4)$$

Ordinary differential equations for the time derivatives of h , T and T_h were obtained by Denman. The derivation of these equations does not change appreciably when salinity is included. The primary effect of including salinity is to alter the term for the turbulent flux of density $\overline{w'\rho'}$. If ρ_0 is the mean density, then

$$\overline{w'\rho'} = \rho_0 (\alpha \overline{w'T'} + \lambda \overline{w'S'}), \quad (5)$$

where $\alpha = \rho_0^{-1}(\partial\rho/\partial T)$ and $\lambda = \rho_0^{-1}(\partial\rho/\partial S)$. Only the case of a deepening mixed layer is considered here, and vertical and horizontal advection have been assumed to be zero. With the inclusion of salinity, the equations of Denman are modified to yield the following system of equations:

those of Denman. Eq. (9) is simply a rearrangement of (4), and Eq. (10) indicates that the salinity profile below the mixed layer is time-independent. A similar derivation for the inclusion of salinity has been independently derived by Kraus and Rooth (1975).

A fundamental assumption of the Denman model is needed to evaluate the wind stress term, $G-D$. Some of the momentum transported into the oceans by the wind stress is assumed to produce turbulent energy on small scales. This turbulent energy is used to increase the potential energy of the water column by doing work against the buoyancy forces. The rate of increase in potential energy of the mixed layer as a result of work done by mixing is assumed to be a constant fraction m of the rate of turbulent energy transferred downward by the wind stress at 10 m above the surface. Hence, $m = -\rho_0 \alpha g (G-D) / (\tau U)$, where g is the gravitational acceleration, τ the surface wind stress, and U the wind speed at 10 m. The constant m will be set equal to 0.0012.

According to Jerlov (1968), the BOMEX region contains water types II and III which have larger extinc-

tion coefficients than the oceanic mean. Hence, the extinction coefficient γ is set at 0.2 m^{-1} unless otherwise specified. Changes in the value of γ will not appreciably change the qualitative nature of the results to be presented. A Runge-Kutta numerical integration scheme with a time step of 3 min is used to solve the system (6)–(10). Results of the computations are presented in the next section.

3. Characteristics of the deepening regime

In this section three different cases in the deepening regime will be considered. Two of the cases will deal with the heating and cooling characteristics of the mixed layer itself, while the other case will deal with the thermal relationship between the mixed layer and the region below. If the mixed layer salinity is greater than the salinity immediately below the mixed layer, convective overturning will occur because of a density instability unless a very rapid temperature decrease occurs across the interface. Only the case of stable salinity stratification will be considered; hence the mixed layer salinity will always be less than the salinity immediately below. Fig. 1 shows a salinity-temperature-density (STD) profile taken in the Atlantic Ocean at $17^{\circ}35'N, 54^{\circ}36'W$ (BOMEX, p. 177). The profile exhibits a sharp increase in salinity at the bottom of a nearly homogeneous mixed layer. Numerical solutions of the system (6)–(10) have been obtained for three different cases using the initial conditions given in Table 1.

Before discussing the numerical results, an analytic solution will be derived which gives an approximate

TABLE 1. Initial values and boundary conditions for the four model cases. The transformation $(R, B, H_e, H_s) = (R_*, B_*, H_{e*}, H_{s*})/(\rho_0 c_p)$ is used to obtain the values used in Eqs. (6)–(10).

	Case 1	Case 2	Case 3	Case 4
h (m)	50	40	20	50
T ($^{\circ}C$)	27.5	28.5	28.1	27.4
T_h ($^{\circ}C$)	27.2	28.4	28	26.9
S ($\% \times 10^3$)	0.03575	0.03375	0.0318	0.0356
S_h ($\% \times 10^3$)	0.0369	0.0353	0.0332	0.0361
L_T ($^{\circ}C \text{ m}^{-1}$)	0.055	0	0.02	0.04
L_s ($\% \text{ m}^{-1} \times 10^3$)	-0.00002	-0.00003	-0.00012	-0.00003
U (m s^{-1})	8	8	6	5
R_* (W m^{-2})	189	97	73	75
H_{e*} (W m^{-2})	85	85	194	136
H_{s*} (W m^{-2})	24	24	24	25
B_* (W m^{-2})	61	73	73	8

expression for the temperature change of the mixed layer as a function of time and depth. This expression will be useful in helping to understand the results of the three cases to be presented. Rearrangement of (7) yields

$$h \frac{dT}{dt} + \frac{dh}{dt} T - \frac{dh}{dt} T_h = Q, \tag{11}$$

where $Q \equiv H_e + H_s + B + R(1 - e^{-\gamma h})$ is the net heating. The temperature gradient L_T is assumed to be fixed, the solar radiation below the mixed layer to be negligible, the initial temperature jump across the bottom interface to be δ , Q to be constant, and h_0 to be the initial depth of the mixed layer. Integration of (8) provides an equation for T_h , which is then substituted in (11). At any time t , the temperature change (ΔT) of the mixed layer is obtained by integrating (11) from $t'=0$ to $t'=t$; this leads to

$$\Delta T = \frac{1}{h} [-F(h) + Qt], \tag{12}$$

where

$$F(h) = (h - h_0) \left[\delta + \frac{L_T}{2} (h - h_0) \right]. \tag{13}$$

The term $F(h)$ is a positive, increasing function of h , representing the cooling of the mixed layer due to entrainment from below. The term Qt represents the heating or cooling of the mixed layer due to the atmospheric fluxes.

a. Case 1

The initial conditions for Case 1 have been chosen to correspond to Fig. 1. Both the temperature and salinity are very nearly constant to a depth of 50 m. The boundary inputs have been chosen to be approximately equal to their annual averages and are held constant for a 10-day integration period. The wind speed U is 8 m s^{-1} . If salinity is not included ($\lambda = 0$), the mixed layer deepens to a depth of 65.6 m at the end of the 10-day period;

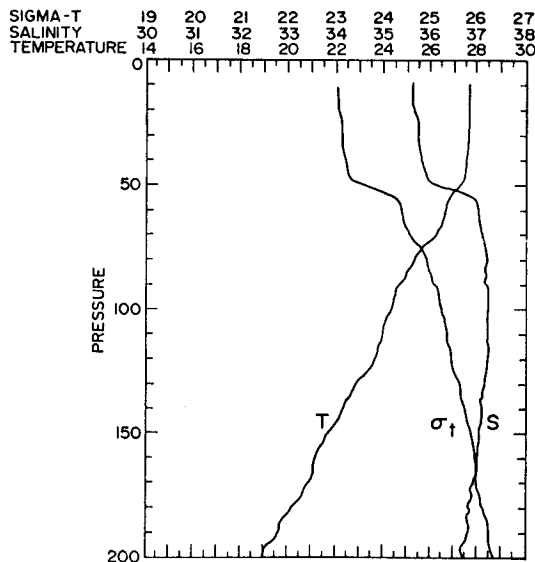


FIG. 1. Observed vertical profiles of temperature, salinity and density. The parameters on the horizontal axis are the density in sigma-t units, the salinity in parts per thousands, and the temperature in $^{\circ}C$. On the vertical axis the pressure in decibars is approximately equal to the depth in meters (BOMEX, p. 177).

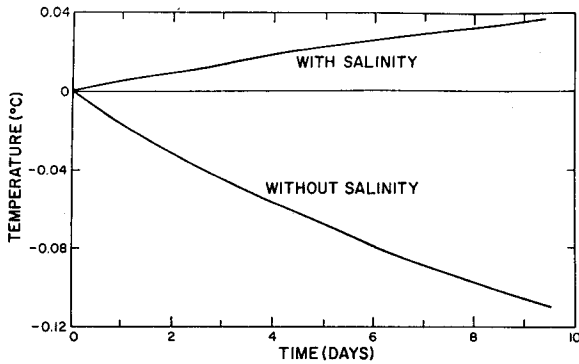


FIG. 2. Model-computed changes of mixed-layer temperatures in Case 1.

with salinity included [$\lambda = 0.7 (\text{‰})^{-1} \times 10^{-3}$], the layer deepens to only 54.9 m. The rapid increase in density at the bottom of the mixed layer in Fig. 1 is due to the salinity jump across the interface. A large density jump significantly slows the deepening rate of the mixed layer because it leads to an appreciable increase in potential energy with only a small amount of deepening.

Fig. 2 shows the change in mixed layer temperature over the integration period. A surprising result emerges! Without salinity the mixed layer temperature decreases; but when salinity is included, the mixed layer temperature actually increases. A physical explanation of this result is as follows. For both cases the net heating at the surface is positive and tends to heat the mixed layer. At the bottom of the layer, however, colder water is being entrained into the deepening mixed layer and tends to cool it. In the case without salinity the cooling due to entrainment is greater than the heating from the surface inputs, and the layer cools. With salinity included, the layer deepens more slowly and entrains less cold water at the bottom. The heating terms dominate, and the mixed layer temperature increases.

The physical explanation can be understood analytically by consideration of (12). If $h_s(t)$ denotes the mixed layer depth when salinity is included and $h_T(t)$ when it is not, then for the same atmospheric inputs $h_s(t) \leq h_T(t)$. This inequality holds for all the cases in this section since inclusion of the salinity jump increases the stability rather than decreasing it. Since $Q > 0$, Eq. (12) indicates that ΔT will be positive whenever $F(h) < Qt$, and ΔT will be negative whenever $F(h) > Qt$. When salinity is not included, the deepening rate is sufficiently large to insure that $F(h_T) > Qt$, and the mixed layer temperature decreases. However, when salinity is included, the left-hand side of the inequality decreases sufficiently such that $F(h_s) < Qt$, and the mixed layer temperature increases.

b. Case 2

Observations from the BOMEX experiment indicate that the layers of thermal and saline homogeneity are

not always the same depth. The initial conditions for Case 2, given in Table 1 and also by the dashed lines in Fig. 3, correspond roughly to an observed profile (BOMEX, p. 122) in which the thermal layer is 52 m deep and the saline layer 40 m. The mixed layer depth is assumed to be the smaller of the two depths, and the temperature gradient immediately below is set equal to zero. A small artificial temperature jump has been inserted at 40 m since a jump is necessary in the numerical calculations when salinity is not included. If the mixed layer deepens below 52 m, the temperature gradient is reset to $0.047^\circ\text{C m}^{-1}$ to reflect the actual thermal conditions.

Other than the different initial profiles, the only difference from Case 1 is a decrease of the solar radiation by a factor of 2; this leads to a net surface cooling. At the end of a 10-day integration period, the mixed layer depth is 89.4 m but if salinity is included the final depth is only 49.8 m. Fig. 3 shows the initial and final profiles for both cases; the temperature decreases for both cases but at a faster rate if salinity is not included. The most interesting result in this case is the development of a mixed layer which is colder than the layer immediately below. If a thermal mixed layer is considered without the effects of salinity, this situation cannot occur because the stratification would be unstable; convective overturning would then occur to readjust the layer. A comparison of Fig. 3 with an

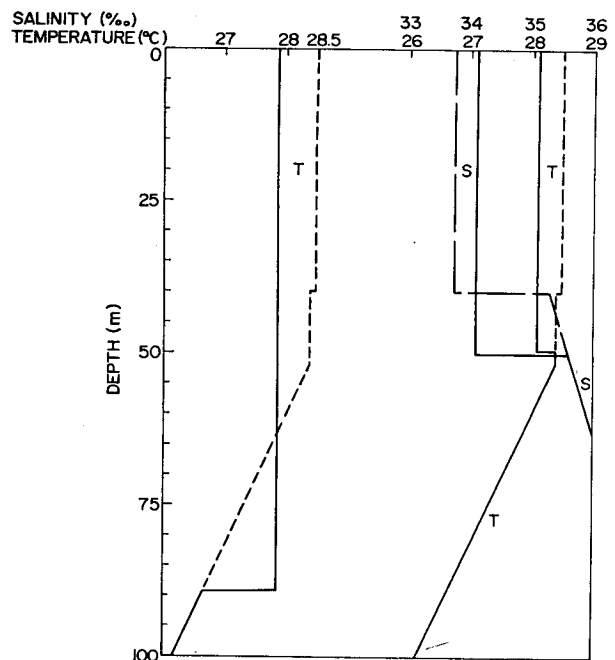


FIG. 3. Comparison of mixed-layer deepening and cooling with and without the effect of salinity. Dashed lines denote the initial temperature and salinity profiles; solid lines denote the profiles after 10 days. The profiles on the left depict the case when salinity is not included, those on the right when salinity is included. The initial temperature profiles are the same for both cases.

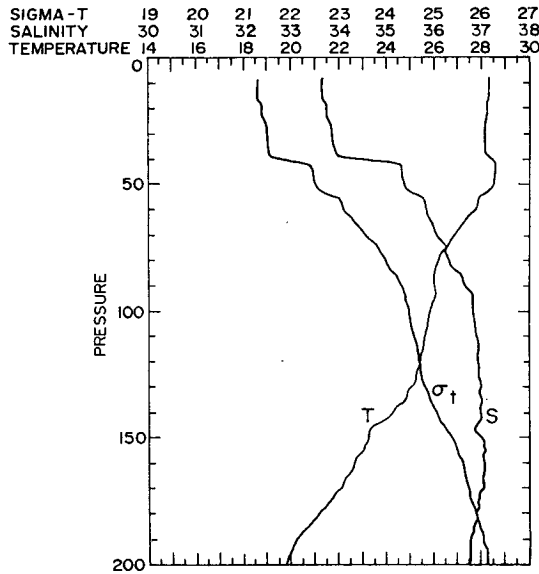


FIG. 4. Vertical profiles of salinity, temperature and density (BOMEX, p. 155).

observed profile in Fig. 4 (BOMEX, p. 155) shows that actual profiles do occur in which an increase in temperature occurs immediately below the layer.

An equation for the time-dependent temperature difference across the bottom interface of the mixed layer can be derived by combining the solution of (8) with $\gamma Re^{-\gamma h} = 0$ and (12) to obtain

$$T - T_h = -\frac{1}{h} \left[\delta h_0 + \frac{L_T}{2} (h - h_0)(h + h_0) + Qt \right]. \quad (14)$$

For the case with salinity effects included, $T - T_h$ is initially positive, but at the end of the integration period $T - T_h < 0$. The numerical results indicate that the mixed layer deepens approximately linearly in time when salinity is included. This linear relationship can be assumed since the salinity jump sufficiently reduces the deepening rate which in turn reduces the nonlinear effects. If the deepening rate r is assumed constant, the time at which the mixed layer temperature first becomes colder than the layer immediately below is given by setting the right-hand side of (14) equal to zero. This yields

$$t \approx -\frac{\delta h_0}{Q + rL_T h_0}. \quad (15)$$

The value of r is obtained from (6) by setting

$$r \equiv \left. \frac{dh_s}{dt} \right|_{t=0}.$$

Substituting the initial conditions into (15), $t = 52.6$ h; this value of t is within 0.5% of the numerical solution. A solution to (15) occurs only if $Q + rL_T h_0 < 0$; hence a determination of whether $T - T_h$ will change sign de-

pends on a relationship between the surface fluxes, the temperature gradient, and the initial depth.

c. Case 3

With the particular choice of boundary and initial conditions in the previous two cases, the mixed layer was found to cool at a faster rate if salinity was not included. The case of a shallow mixed layer with a large salinity jump at the bottom and strong surface cooling will now be considered. The specification of the initial profile in Table 1 corresponds to an observed profile (BOMEX, p. 270). The integration period is again 10 days. Initially, the cooling rate is greater without salinity as in the previous two cases, but after 5 days the cooling rate is greater with salinity.

The cooling rate without salinity will be greater than when salinity is included if the following inequality derived from (12) is satisfied:

$$\delta h_0 + Qt + \frac{L_T}{2} (h_T h_s - h_0^2) > 0. \quad (16)$$

Since the mixed layer is initially only 20 m deep and Q is negative with a large magnitude, the term Qt dominates after approximately 140 h, and the above inequality reverses. A physical explanation can be based on changes in total heat content over layers of different depths. Since the salinity effect reduces the depth of the mixed layer, the heat loss occurs over a thinner layer than if the salinity jump were absent. Hence, the temperature decrease for a given heat loss would be greater when the salinity effect is included. The increase in surface salinity is about 1.1‰, of which about 5% is due to the large evaporative heat flux ($E \approx 0.7$ cm day⁻¹).

4. Effects of precipitation

Salinity and temperature changes occur at the sea surface during periods of precipitation. The nature of these changes is not well understood. Ostapoff *et al.* (1973) have detected salinity changes in tropical oceans of about 0.15‰ over a large area of steady rainfall during an 18 h period. Efforts by Elliott (1974) to determine precipitation rates over the ocean by measuring the changes in surface salinity at 1 h intervals were less successful. He found that during periods of no rain, salinity regularly fluctuated by ± 0.15 ‰ and that such fluctuations tended to obscure salinity depressions due to rainfall. He also found, however, that if the sampling intervals were taken at 6 min intervals, short-term salinity depressions were visible. In this section the effects of precipitation will be investigated numerically using the observational data of Ostapoff *et al.* for a comparison.

In Denman's model, transition from a wind to a heat regime occurred whenever the numerator of (6) became

TABLE 2. Effects of precipitation on the model results. Atmospheric fluxes are listed under Case 4 of Table 1. A total precipitation of 45 mm falls uniformly throughout the period of rainfall. The maximum temperature and salinity changes in the surface layer are denoted by ΔT_{\max} and ΔS_{\max} , respectively. The new mixed layer forms at a depth h_p . It persists for a time t_p , which is assumed to be the time at which the salinity jump at the bottom of the mixed layer falls below 0.1‰.

	Dura- tion of rain- fall (h)	ΔT_{\max} (°C)	ΔS_{\max} (‰)	h_p (m)	t_p (h)
$U = 5 \text{ m s}^{-1}$	4	0.76	2.0	0.76	15
	15	0.31	0.24	6.2	5
$U = 10 \text{ m s}^{-1}$	4	0.09	0.26	6.0	5
	15	0.04	0.04	38.1	0

negative. A new, shallower mixed layer then formed at a depth which was determined by setting the numerator of (6) equal to zero and solving for h . The same procedure is followed here for the case of a precipitation regime. If the mixed layer is deepening and there is no precipitation ($P=0$), then the initiation of rainfall ($P>0$) will change the sign of (6) from positive to negative. The numerator of (6) is then set equal to zero and solved for h . This value of h is assumed to be the depth to which the new stable layer formed by the precipitation is mixed by the turbulent fluxes. The changes in salinity and temperature will be determined from (7) and (9) with $dh/dt=0$, and T_h and S_h will be fixed at the surface values of T and S at the onset of precipitation. The value of T_h can continue to increase due to radiation which penetrates below the new mixed layer; it will be assumed that this radiation is distributed uniformly throughout the depth of the mixed layer which existed prior to the onset of precipitation. Time steps in the precipitation regime are taken to be 1 h.

The fluxes for Case 4 of Table 1 correspond to those observed by Ostapoff *et al.* for an 18 h period in July at 5°N, 21°W. A total rainfall of 45 mm is assumed to fall uniformly during the first 15 h of this period. The extinction coefficient γ is set equal to 0.1 m^{-1} , and the solar radiation assumes the value given in Table 1 for 12 h, starting at the onset of precipitation; otherwise, $R=0$. The results of Case 4 will now be discussed.

Initially the mixed layer is deepening slowly; then at 0900 GMT precipitation begins, and the model predicts the formation of a new mixed layer at 6 m. After 15 h the precipitation stops, and the model reverts to a deepening regime. The observations taken 18 h after the onset of precipitation indicate the formation of an 11 m mixed layer with a temperature and salinity decrease of 0.2°C and 0.164‰ , respectively. The model results produce a 10 m mixed layer with temperature and salinity decreases of 0.24°C and 0.15‰ , respec-

tively. At the end of the precipitation period, however, the model mixed layer depth is only 6.2 m; hence much of the agreement between the model and observation is due to the deepening which occurred during the 3 h period after the cessation of rainfall.

The depth at which the new mixed layer forms during the precipitation regime is quite sensitive to the value of the parameter m which was defined in Section 2. This empirically determined parameter represents the fraction of the energy generated by the surface winds which appears as turbulent fluxes in the ocean mixed layer. The value of m in this paper has been assumed to be independent of wind speed and mixed layer depth. For shallow mixed layers which occur in the precipitation regime, the transfer of energy might be more efficient, and the value of m might be larger. More observational information during periods of precipitation would be useful for verification.

When precipitation occurs in conjunction with high surface winds, the new mixed layer is deeper than at lower wind speeds. Also, for a given total amount of precipitation, the depth of the newly formed stable layer depends on the duration of rainfall. Table 2 lists the surface characteristics for a fixed total rainfall (45 mm) over different periods of time and for different surface wind speeds. The results of Case 4 are included in the table. The table shows that the occurrence of light precipitation accompanied by large surface winds cannot be detected by changes in surface salinity or temperature. However, heavy rainfall accompanied by light winds can lead to temperature and salinity decreases of 0.76°C and 2.0‰ , respectively.

Although sufficient data have not been presented to document the quantitative results of this section, the qualitative results are of interest. The formation of a new stable layer as a result of precipitation has been observed. The net surface cooling then acts over a thinner layer, which leads to a greater decrease in sea surface temperature. The cooling of the sea surface would tend to decrease the fluxes of latent and sensible heat into the atmosphere and reduce the amount of moisture that enters the atmosphere. This negative feedback could be useful in a coupled ocean-atmosphere model as a cutoff mechanism for precipitation over tropical oceans.

5. Conclusions

The work in this paper was originally motivated by the desire to couple a relatively simple mixed layer ocean model to a global atmospheric general circulation model for the purpose of predicting seasonal weather anomalies. Accurate sea surface temperatures must be provided to the atmospheric model for such predictions. Denman and Miyake have shown that, at least in one case, sea surface temperatures can be accurately determined using a thermally homogeneous mixed layer model. The results presented here (neglecting the

effects of upwelling and horizontal advection) show that the presence of a homogeneous saline layer can have a significant effect on the depth and temperature of the mixed layer.

In general, the deepening of the mixed layer occurs when the turbulent energy produced by the surface stresses works against the density gradient to increase the potential energy of the mixed layer. The most important difference which arises when the mixed layer has a salinity jump as well as a temperature jump at the bottom is the formation of a larger density jump across the interface. The increased density jump causes the mixed layer to deepen more slowly, which leads to a change in the heating and cooling characteristics of the mixed layer.

The most significant thermal effect produced by the inclusion of salinity is the tendency to reduce the cooling rate of the mixed layer due to entrainment across the bottom interface. In Case 1 the reduced entrainment of cold water at the bottom interface enables the positive net heat inputs at the surface to actually warm the mixed layer; when salinity was not included, there was sufficient entrainment to cool the mixed layer. Hence, in some cases the thermal effect due to salinity will be such as to result in the correct sign for the temperature change of the mixed layer.

The presence of a salinity jump at the bottom interface in conjunction with a significant net cooling at the air-sea interface can lead to the development of a mixed layer which is cooler than the region immediately below. Observed profiles such as in Fig. 4 confirm that such situations do occur. This situation would not occur if only a thermal mixed layer were considered, since the layer would then be unstable and convective overturning would cause the region below to cool.

Whenever there is a net cooling at the sea surface, a deepening regime occurs, and two different mechanisms contribute to the cooling of the mixed layer. The net heat loss at the surface cools the layer, and the entrainment of colder water as the layer deepens also leads to cooling. If a shallow mixed layer with a large salinity jump at the bottom interface is exposed to large surface cooling, the inclusion of salinity effects can lead to a faster cooling rate in the mixed layer. In this case the cooling is dominated by the surface fluxes. Hence, the

inclusion of salinity effects can lead to either an increase or a decrease in the cooling rate of the mixed layer, depending on whether the surface fluxes or the entrainment is the dominant cooling mechanism.

The occurrence of heavy precipitation over tropical oceans leads to the development of a stable oceanic mixed layer at the ocean surface. The ability to detect significant changes in the surface temperature and salinity fields depends on the precipitation rate, the wind speed, and the atmospheric fluxes. During periods of rainfall, heat losses are restricted to this newly formed stable layer, and significant decreases in surface temperature as well as salinity can occur. This decrease in sea surface temperature may be important in a coupled ocean-atmosphere model. The temperature drop would lead to a decrease of the latent heat flux into the atmosphere thus providing a negative feedback mechanism for precipitation over tropical oceans.

Acknowledgments. The author would like to thank Prof. P. H. Stone for his comments on the manuscript. The research was supported through a NAS-NRC Resident Research Associateship at the Goddard Institute for Space Studies, NASA, New York, N. Y.

REFERENCES

- Defant, A., 1961: *Physical Oceanography*, Vol. I. London, Pergamon Press, 729 pp.
- Denman, K. L., 1973: A time-dependent model of the upper ocean. *J. Phys. Oceanogr.*, **3**, 173-184.
- , and M. Miyake, 1973: Upper layer modification at Ocean Station "Papa": Observations and simulation. *J. Phys. Oceanogr.*, **3**, 185-196.
- Elliott, G. W., 1974: Precipitation signatures in sea-surface-layer conditions during BOMEX. *J. Phys. Oceanogr.*, **4**, 498-501.
- Jerlov, N. G., 1968: *Optical Oceanography*. Amsterdam, Elsevier, 194 pp.
- Kraus, E. B., and C. Rooth, 1975: Oceanographic modelling for atmospheric predictions. To appear in *Modelling and Prediction of the Upper Layers of the Ocean*, NATO Advanced Study Institute, Urbino, Italy.
- , and J. S. Turner, 1967: A one-dimensional model of the seasonal thermocline II. The general theory and its consequences. *Tellus*, **19**, 98-106.
- Ostapoff, F., Y. Tarbeyev and S. Worthem, 1973: Heat flux and precipitation estimates from oceanographic observations. *Science*, **180**, 960-962.
- U. S. Dept. of Commerce, NOAA, 1972: *BOMEX Period III Upper Ocean Soundings*. Rockville, Md., 352 pp.